31st Annual International Conference of the IEEE EMBS
Minneapolis, Minnesota, USA, September 2-6, 2009

Linear Control of Neuronal Spike Timing Using Phase Response Curves

Tyler Stigen, Per Danzl, Jeff Moehlis, Theoden Netoff

Abstract—**We propose a simple, robust, linear method to control the spike timing of a periodically firing neuron. The control scheme uses the neuron's phase response curve to identify an area of optimal sensitivity for the chosen stimulation parameters. The spike advance as a function of current pulse amplitude is characterized at the optimal phase and a linear least-squares regression is fit to the data. The inverted regression is used as the control function for this method. The efficacy of this method is demonstrated through numerical simulations of a Hodgkin-Huxley style neuron model as well as in real neurons from rat hippocampal slice preparations. The study shows a proof of concept for the application of a linear control scheme to control neuron spike timing in-vitro. This study was done on an individual cell level, but translation to a tissue or network level is possible. Control schemes of this type could be implemented in a closed loop implantable device to treat neuromotor disorders involving pathologically neuronal activity such as epilepsy or Parkinson's disease.**

I. INTRODUCTION

In this study, we consider controlling the spike timing of a periodically firing neuron. This approach uses a single stimulation pulse per firing period to control the spike timing. We use the neuron's phase response curve (PRC) to determine the timing of the stimulation pulse [1]. A PRC is a measurement in periodic systems of how a perturbation advances the next event as a function of the phase [3].

The goal is to create a robust algorithm to control the spike timing of a periodically firing neuron and, by extension, to control the level of synchrony in a population of periodically firing neurons. Neuromotor diseases such as Parkinson's disease (PD) and epilepsy are caused by increased or decreased synchrony of neuronal firing. Recent studies have shown that symptoms of both PD and epilepsy can be treated using a procedure known as electrical deep brain stimulation (DBS) [2, 3, 4]. Current technology for DBS uses open loop stimulation algorithms to deliver high frequency stimulus pulses to the brain through implanted electrodes. The Food and Drug Administration has approved DBS for use in PD and several other motor disorders. It is expected that DBS for treatment of epilepsy will be approved by 2012. Much as cardiac pacing evolved from open loop stimulation to closed loop stimulation, DBS is currently transitioning from using open loop stimulation to closed loop stimulation. Closed loop stimulation devices are desirable because energy consumption is reduced and unnecessary stimulation of the patient is reduced. This leads to longer service life for the device and fewer side effects for the patient. We envision the algorithm presented here being integrated in a closed loop implantable DBS system that would sense synchronization of neuronal firing and appropriately stimulate to synchronize or desynchronize the population preventing the associated pathological symptoms [5, 6].

Manuscript received June 20, 2009.

Theoden Netoff is with the University of Minnesota, Minneapolis, MN 55455 USA (corresponding author phone: 612-216-5002; e-mail: tnetoff@umn.edu).

Tyler Stigen is with the University of Minnesota, Minneapolis, MN 55455 USA (e-mail: stig0022@umn.edu).

Per Danzl is with the University of California Santa Barbara, Santa Barbara, CA 93106 USA(e-mail: pdanzl@engineering.ucsb.edu)

Jeffrey Moehlis is with the University of California Santa Barbara, Santa Barbara, CA 93106 USA(e-mail: moehlis@engineering.ucsb.edu)

II. METHODS

A. Biological Preparation

All experiments were conducted as approved by the University of Minnesota Institutional Animal Care and Use Committee. Solutions and slice preparation used in biological preparation is detailed in references [3, 7]. Whole cell patch clamp recordings were done in the CA1 region of hippocampus and medial entorhinal cortex (MEC) with both pyramidal and stellate cells.

B. Dynamic Clamp Setup

Only neurons that maintained a resting membrane potential between -50 and -70 mV with less than -300 pA of holding current were used. Cells were further selected based on their ability to spike periodically when driven by the spike rate controller. The membrane potential was amplified and low-pass filtered at 1 KHz using the Axon 700B amplifier then relayed to a computer running a real-time Linux interface. The closed loop neuronal firing rate control and experimentation was done using the Real Time Experimental Interface (RTXI, www.rtxi.org) and dynamic clamp techniques described by Dorval et al. [8]. RTXI is a framework for creating custom real-time modules in C++, such as a spike rate controller to dynamically control current input to maintain a target inter-spike interval. By modularizing simple applications, complex processes can be created easily by interconnecting various modules. Custom modules for RTXI were written in C++ to control the periodic spiking of the neuron, simulate a Hodgkin-Huxley neuron, construct PRCs, estimate parameters, and execute and verify the control algorithm, Figure 1. The dynamic clamp combines patch clamp recording techniques with a computer to allow for closed loop interaction with the neuron. Patch clamping involves attaching a micrometer diameter glass pipette to a neuron to allow for direct intracellular measurement of the neurons membrane potential.

C. Model Neuron

The real-time model neuron used for simulation in the dynamic clamp is a Hodgkin-Huxley type conductance based model [9]. The governing equation is seen below.

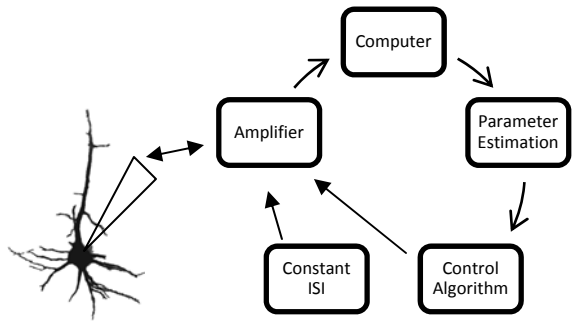

Fig. 1. Schematic of experimental setup. A neuron is whole cell patch clamped. The membrane potential is amplified and sent to a computer running a real-time Linux kernel. Using RTXI, custom modules calculate the necessary current to maintain periodic firing, construct the neuron's PRC, estimate the parameters and implement the control algorithm.

$$C\frac{dV}{dt} = g_{Na}m^3h(V - E_{Na}) + g_K n^4(V - E_K) + g_L(V - E_L) + I$$

The model uses sodium, potassium, and leak conductances internally and can also accept direct current (I) input from other Dynamic clamp modules. The model was integrated with a Runge-Kutta 4 integrator at 40 kHz.

D. Linear Control Methodology

The objective of the control algorithm is to control the neurons spike timing to an arbitrary advance or delay using only a single pulse per period. The first step in the control scheme is to choose stimulation parameters. The shape of the stimulation pulse can be of arbitrary complexity, but in this study, square wave pulses with 0.2 ms pulse width were used. It should be noted that the subsequent optimization is dependent on the shape and width of the stimulation selected. The next step is to determine the optimal time in which to stimulate the neuron to provide optimal control. We can determine this value by constructing a PRC for the neuron. The phase of the neuron is defined as the interval (0,1), with 0 corresponding to the neuron spiking and 1 corresponding to the next time the neuron spikes. As such, one complete phase is equal to the inter-spike interval (ISI). If the phase is not normalized to 1, the phase response curve is also known as the Spike Time Response Curve (STRC)[3]. The PRC can be constructed for a periodically firing neuron by inputting a stimulation pulse at a given point in the phase and recording the phase advance or delay caused by that input and repeating for every possible input point in the phase. In figure 2, two identical stimulation pulses are delivered at two different points in the period. While one pulse early in the phase creates a small delay, another late in the phase creates a large advance. By plotting the response of the neuron at each phase and fitting a curve to the data we estimate the PRC of the neuron. In figure 2B, we show a typical function representing PRC. The maximum value of the PRC will describe the most sensitive phase, $\varphi_{opt,}$ in the period to the stimulus used. The optimal stimulation time,

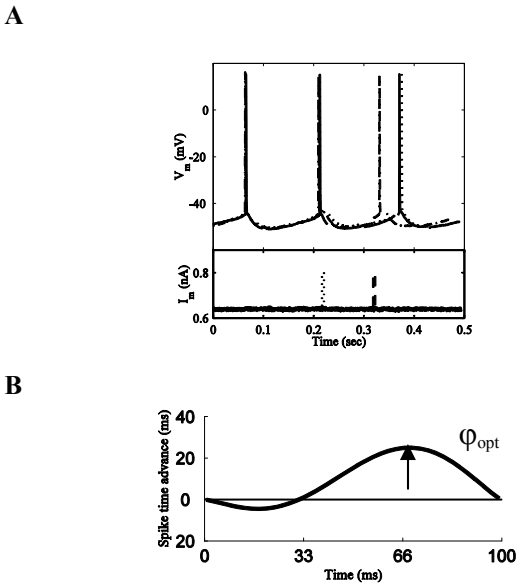

Fig. 2. A: Inputs at different points in the phase can produce advance or delay of different magnitudes. B: The STRC derived from the PRC, with the optimal time for stimulation indicated. Modified from Netoff{{1 Netoff,T.I. 2005}}.

$T_{opt} = \varphi_{opt} \cdot ISI$. Next, we characterize the relationship of spike advance and stimulation pulse amplitude at T_{opt}. While the PRC was slightly different for each neuron, we found that φ_{opt} =0.7 was sufficient in all cases tested. We chose this value because the maximum value of the PRC generally lies in the range of φ_{opt} = 0.6-0.8, the derivative of the PRC in that range is generally flat, and it allows for both advance and delay of the spike time. Additionally, this control algorithm does not require that the stimulus be applied at the most sensitive phase. The selection of φ_{opt} could be arbitrary, but a judicious choice that allows for both advance and delay is desirable from a utility standpoint.

We inject current pulses of the same width applied at the same phase, but random amplitudes to characterize the advance or delay of the spike time. Plotting this advance or delay against the amplitude of the input creates an advance vs. current map (AVC map). The AVC map is the basis behind the linear control, as it describes the effect of all possible amplitudes of positive and negative stimulus at φ_{opt}. This map is fit with a linear least squares regression. By inverting the regression line, we create the linear control function, which will generate the appropriate stimulus strength for a given target spike advance.

III. RESULTS

Using RTXI, a Hodgkin-Huxley type neuron model was used to test the control process [11]. Constant current was injected to drive the neuron driven to fire with an ISI = 100 msec. The constant current was adjusted to maintain the firing rate using a PID controller. The PRC was estimated first and the optimum phase was determined to be φ_{opt} =0.7. Using this phase, we next measured the AVC map, shown in

Figure 3.

A. Model Neuron Results

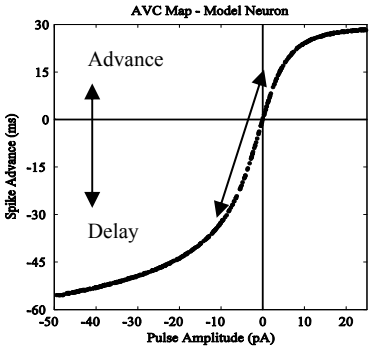

Fig. 3. The Advance vs. Current map has a characteristic sigmoid shape. It is generated using a range of current values input at the optimum phase. The lower left quadrant contains the spike delay and the upper right quadrant contains the spike advance. The sigmoid has a linear region that is used as the control domain.

The AVC map has a distinct sigmoid shape in the model neuron as seen in Fig. 3. Due to causality, the neuron reaches a maximum advance of ISI-T_{opt} in the upper right quadrant. This represents the stimulus pulse eliciting a spike versus advancing the spike time. The spike delay of the neuron is limited only by how much negative current the neuron can accept. As the AVC map is sigmoid in shape, it does not lend itself to accurate control by a linear function. However, the sigmoid curve does have a linear region as indicated in Fig.3. The linear region represents a domain that contains both spike advance and delay, as such; it is the logical region to use for fitting the linear control function. The efficacy of the control was evaluated by comparing target spike advance to the recorded spike advance as seen in Fig. 4. The correlation (R) and slope (M) of the control accuracy plot were used as statistical measures. Perfect control statistics would be R=1 and M = 1, indicating that the target spike advance or delay was achieved exactly with no variance. The model neuron statistics were R=0.99 and M = 1.09.

A. Real Neuron Results

The AVC map of a real neuron (Fig. 5) has significantly more noise than was seen in the model neuron. The sigmoid shape is nearly impossible to recognize. In the upper right quadrant, we see that the stimulus probabilistically elicits spiking due to the increased variability. In the real neuron, it appears the linear function would reasonably describe the entire range of spike advance and delay values. The AVC map of the real neuron has much higher variance than the model neuron. By plotting the target advance against the actual advance, we can see that there is a high correlation, Figure 6. As expected, the real neuron has significantly higher variability and as such the actual advance follows the target advance less precisely than in the simulated neuron.

A

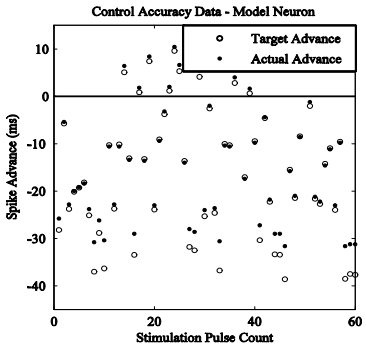

B

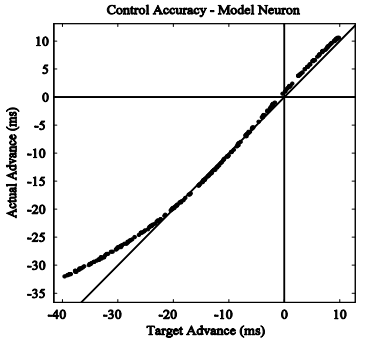

Fig. 4. A: The control accuracy data for the model neuron shows the first 60 random target advance times and the actual times. The actual advance was within 1, 5, and 10 ms of the target advance in 52, 90, and 100 % of the time respectively. B: The control accuracy plot showing the target advance with actual advance for the model neuron. The line is unity. At longer delays, outside of the linear domain, the control becomes less accurate.

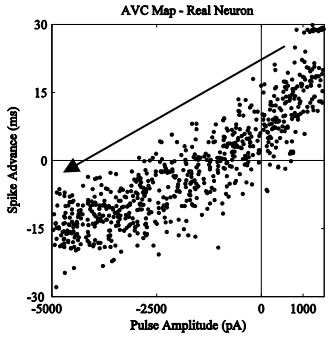

Fig. 5. The Advance vs. Current map in a real neuron loses much of its characteristic sigmoid shape. The noise of a real neuron allows the linear control scheme to fit the mean of the data quite accurately.

Five neurons from five subjects were tested in the manner described above. The control accuracy statistics can be found in the Table.

IV. Discussion

The neuronal control algorithm presented here is meant to control an individual periodically firing neuron, but we believe it can be extended for use in populations of neurons as well. While this method is mathematically simple, it is robust to noise and inaccuracies in the estimate of the phase of the neuron.

A

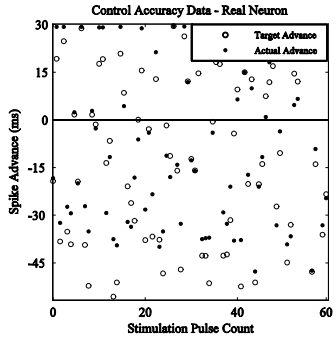

B

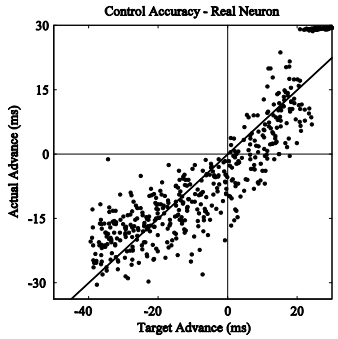

Fig. 6. A: The control accuracy data for the model neuron shows the first 60 random target advance times and the actual times. The actual advance was within 1, 5, and 10 ms of the target advance in 7, 32, and 55 % of the time respectively. B: The control accuracy plot showing the target advance with actual advance for the model neuron. The line is unity.

Controlling neuronal firing using PRC-derived linear control appears to be quite accurate considering the variability of inter-spike intervals in mammalian neurons. The spike delay range is much greater in almost all cases. Controlling spike timing using inhibitory input does not seem to have a well defined limit as seen in spike time advance. Since the spike advance is limited to a fraction of the period, the delay, which can be greater than one period, allows for a larger range of spike time control. Another promising finding is that the control function coefficients were very similar in value across multiple neurons. This indicates that it might be possible to use the same coefficients across multiple neurons, as shown in the Table. Additionally, the control accuracy statistics remained similar over several neurons from different subjects. Combined, these findings show promise for population level control using the proposed method. Much of the variability in the control of these neurons can be attributed to two main sources, intrinsic neuronal variability and firing rate controller noise. The firing rate controller used to drive the neurons to fire periodically is not perfect. It induces some current offset that the system cannot properly account for at this time. Ongoing work using a new PID-based firing rate controller and sigmoid control function has shown some promise and warrants further exploration.

TABLE: CONTROL ACCURACY STATISTICS

Cell	R	M	A	B
Cell 1	0.923	0.981	1.11E-07	-1.44E-09
Cell 2	0.928	1.136	1.36E-07	-1.35E-09
Cell 3	0.966	0.837	1.48E-07	-1.61E-09
Cell 4	0.948	0.958	3.44E-07	-1.55E-09
Cell 5	0.918	1.230	2.15E-08	-4.41E-12
μ	0.936	1.020	1.52E-07	-1.19E-09
σ	0.019	0.153	1.18E-07	6.72E-10

R is the correlation coefficient of the control accuracy plot data. M is the slope of least-squares linear regression for the control accuracy plot data. Coef A and Coef B are the coefficients for control function of the form, I=A (Advance) +B. μ is the mean. σ is the standard deviation.

References

[1] B. S. Gutkin, G. B. Ermentrout and A. D. Reyes. (2005, Aug). Phase-response curves give the responses of neurons to transient inputs *J. Neurophysiol. 94(2),* pp. 1623-1635.

[2] A. L. Benabid, P. Pollak, C. Gervason, D. Hoffmann, D. M. Gao, M. Hommel, J. E. Perret and J. de Rougemont. (1991, Feb 16). Long-term suppression of tremor by chronic stimulation of the ventral intermediate thalamic nucleus *Lancet 337(8738),* pp. 403-406.

[3] T. I. Netoff, M. I. Banks, A. D. Dorval, C. D. Acker, J. S. Haas, N. Kopell and J. A. White. (2005, Mar). Synchronization in hybrid neuronal networks of the hippocampal formation *J. Neurophysiol. 93(3),* pp. 1197-1208.

[4] A. A. Kuhn, A. Tsui, T. Aziz, N. Ray, C. Brucke, A. Kupsch, G. H. Schneider and P. Brown. (2009, Feb). Pathological synchronisation in the subthalamic nucleus of patients with parkinson's disease relates to both bradykinesia and rigidity *Exp. Neurol. 215(2),* pp. 380-387.

[5] P. A. Tass. (2003, Aug). A model of desynchronizing deep brain stimulation with a demand-controlled coordinated reset of neural subpopulations *Biol. Cybern. 89(2),* pp. 81-88.

[6] P. A. Tass. (2002, Aug). Desynchronization of brain rhythms with soft phase-resetting techniques *Biol. Cybern. 87(2),* pp. 102-115.

[7] J. R. Moyer Jr and T. H. Brown. (1998, Dec 31). Methods for whole-cell recording from visually preselected neurons of perirhinal cortex in brain slices from young and aging rats *J. Neurosci. Methods 86(1),* pp. 35-54.

[8] A. D. Dorval, D. J. Christini and J. A. White. (2001, Oct). Real-time linux dynamic clamp: A fast and flexible way to construct virtual ion channels in living cells *Ann. Biomed. Eng. 29(10),* pp. 897-907.

[9] A. L. HODGKIN and A. F. HUXLEY. (1952, Aug). A quantitative description of membrane current and its application to conduction and excitation in nerve *J. Physiol. 117(4),* pp. 500-544.